Virus Research 259 (2019) 68–76

Contents lists available at ScienceDirect

Virus Research

journal homepage: www.elsevier.com/locate/virusres

Dengue virus potentially promotes migratory responses on endothelial cells by enhancing pro-migratory soluble factors and miRNAs

Diego Alejandro Álvarez-Díaz[a], Aimer Alonso Gutiérrez-Díaz[b], Elizabeth Orozco-García[a], Andrés Puerta-González[a,b], Clara Isabel Bermúdez-Santana[b], Juan Carlos Gallego-Gómez[a,*]

[a] Grupo Medicina Molecular y de Translación – Facultad de Medicina, Universidad de Antioquia, Medellín, 050010, Colombia
[b] RNómica Teórica y Computacional – Facultad de Ciencias, Universidad Nacional de Colombia, Bogotá, 111321, Colombia

ARTICLE INFO

Keywords:
Dengue virus
Endothelial cells
Cytokines
Cell migration

ABSTRACT

The most life-threatening effect of the Dengue virus (DENV) infection is an acute destabilization of the microvascular endothelial cell (MEC) barrier leading to plasma leakage, hypovolemic shock and haemorrhage. However, the underlying cellular mechanisms responsible for the dysfunction of MECs are not well understood. To identify potential cellular processes altered during DENV infection of MECs, expression profiles of cytokines/growth factors and microRNAs were measured by Luminex assay and next generation sequencing, respectively. Synchronously DENV2-infected MECs increase the secretion of IL-6, IL-8, FGF-2, GM-CSF, G-CSF, TGF-α, GRO, RANTES, MCP-1 and MCP-3. Conditioned media of infected MECs increased the migration of non-infected MECs. Furthermore, six miRNAs deregulated at 24 hpi were predicted to regulate host genes involved in cell migration and vascular developmental processes such as angiogenesis. These *in silico* analyses provide insights that support that DENV promotes an acute migratory phenotype in MECs that contributes to the vascular destabilization observed in severe dengue cases.

1. Introduction

Dengue viruses, classified into four serotypes (*DENV*1-4), are the etiological agents responsible for the potentially fatal disease known as severe dengue (SD). It is estimated that up to 3.9 billion people are at risk of being infected with *DENV* (Bhatt et al., 2013). Each year, 284–528 million infections and approximately 250,000 to 500,000 cases of SD are reported worldwide (WHO, 2017). Dengue pathogenesis is shaped by a complex interplay between virus virulence, the host genetic background and the host immune system (Bäck and Lundkvist, 2013). However, the hallmark of SD emerges from a serious vascular involvement that leads to the vascular leakage one of most life-threatening signs of SD (St John et al., 2013; WHO, 2009).

The endothelial cell lining of the microvasculature plays a central role in regulating vascular permeability; this cellular barrier is disrupted in several organs of SD patients although immunohistochemical analyses of endothelium suggest that vascular leakage occur without major morphological damage to the capillary endothelium (Malavige and Ogg, 2017). It has been reported that infectious dengue viruses are commonly isolated from human sera samples in acute infections, suggesting that endothelial cells (ECs) and *DENV* are in close contact *in vivo* (Srikiatkhachorn et al., 2012). In addition, *in vitro* studies have proposed that *DENV* infects human umbilical ECs via interaction with heparan sulfate-containing cell surface receptors, and *DENV*-infected ECs release several soluble mediators involved in the enhancement of immune responses and capillary permeability including IL-6, IL-8, CXCL9, CXCL10 and CXCL11 (Dalrymple and Mackow, 2012). However, other studies suggest that ECs despite being important sources of soluble mediators are poorly infected by *DENV* and are not important targets for *DENV* replication (Calvert et al., 2015; Talavera et al., 2004; Zamudio-Meza et al., 2009).

Several studies have reported increased levels of cytokines and growth factors (GFs), such as VEGF, GM-CSF, Angiopoietin 2, IFNα, IFNγ, IL-6, IL-8, IL-10, CXCL9, CXCL10, CXCL11, MIF, TNF-α and MCP1, in *DENV*-infected patients and ECs culture supernatants (Dalrymple and Mackow, 2012; Michels et al., 2012; St John et al., 2013; Tramontini Gomes de Sousa Cardozo et al., 2017). Among these soluble factors, VEGF, GM-CSF, Angiopoietin 2, IL-8, MCP1 CXCL9, CXCL10 and CXCL11 are known as potent stimulators or inhibitors of endothelial cell migration which is an early step of angiogenesis. During

* Corresponding author at: Universidad de Antioquia – Facultad de Medicina Carrera, 51 D No. 62 - 29. Edificio MUA, Oficina. 303, Medellín, 050010, Colombia.
E-mail addresses: daalvarezd@unal.edu.co (D.A. Álvarez-Díaz), aiagutierrezdi@unal.edu.co (A.A. Gutiérrez-Díaz), elizabeth.orozco@udea.edu.co (E. Orozco-García), andres.puertag@udea.edu.co (A. Puerta-González), cibermudezs@unal.edu.co (C.I. Bermúdez-Santana), carlos.gallego@udea.edu.co (J.C. Gallego-Gómez).

https://doi.org/10.1016/j.virusres.2018.10.018
Received 2 September 2018; Received in revised form 21 October 2018; Accepted 23 October 2018
Available online 25 October 2018

angiogenesis, new blood vessels are formed from pre-existing ones, implying a transitory destabilization of the endothelium through the weakening of tight and adherent junctions between ECs (Tu et al., 2015). Thus, the interaction DENV-MECs independent of the level of infection could promote vascular responses such as endothelial cell migration that can contribute to *DENV*-induced vascular dysfunction.

In addition to cytokines and growth factors, other cellular products such as miRNAs can influence the endothelial cell migration (Wu et al., 2009), and several host miRNAs are deregulated in numerous viral infections including DENV (Liu et al., 2016; Zhu et al., 2014). The involvement of deregulated miRNAs during DENV-infection on EC migration has not been contemplated although there is evidence of other viruses responsible for vascular permeability-based diseases in which infection alters the expression of miRNAs with important roles in EC migration, adherence, and angiogenesis (Pepini et al., 2010).

Finally, although cytokines and growth factors responses from EC to DENV-infection have been documented (Dalrymple and Mackow, 2012; Talavera et al., 2004), the potential role of conditioned media from these cells as a migratory stimulus for non-infected ECs has not been evaluated. Based on the expression profiles of cytokines and growth factors, as well as the evaluation miRNAs profiles in DENV-infected microvascular ECs, in this work it is hypothesized that DENV promotes an acute migratory phenotype in MECs that contributes to the vascular destabilization observed in SD.

2. Materials and methods

2.1. Cell lines and synchronized infections

Dengue virus serotype 2 New Guinea Strain (DENV-2 NGS) was propagated in C6/36 cells (ATCC, CRL-1660™). Virus stocks and supernatants were titrated by plaque lysis assays in Vero cells - ATCC (CCL-81™) as described (Martinez-Gutierrez et al., 2014). HMEC-1 cells (human dermal microvascular endothelial cells) provided by Francisco Candal (CDC - Atlanta, GA, USA) were seeded on porcine gelatin-coated crystals and incubated overnight at 37 °C and 5% CO_2 in basal growth medium (MCDB131 medium supplemented with 2 mM L-glutamine, 0.5% of FBS and deprived of hEGF and hydrocortisone). DENV2 was added to the cell monolayers at a multiplicity of infection (MOI) of 10 and virus binding was synchronized on ice for 30 min. Cells and supernatants were collected at 1, 3, 6, 12, 24 and 48 h post-infection (hpi). Time-matched assays with mock-infected cells with supernatants of non-infected C6/36 cells were also performed.

2.2. LDH assay

Active lactate dehydrogenase (LDH) enzyme levels in culture supernatants from 1, 3, 6, 12, 24, 36 and 48 hpi were evaluated using the Lactate Dehydrogenase (LDH) Cytotoxicity Detection Kit (Roche, Zurich-Switzerland) according to the manufacturer's instructions as a measure of cell viability percentage. Absorbance (Abs) of three diluted (1/5), replicated samples was measured at 490 nm in a plate reader (iMark™ Microplate Absorbance Reader –Bio-Rad), and cell viability over time was calculated for infected and mock-infected cells after Abs subtraction of culture media alone using the following formula: (Abs of culture supernatants / Abs of culture supernatants from Triton X-100 lysed cells)*100.

2.3. Fluorescence microscopy and image processing

DENV-infected and mock-infected HMEC-1 cells were processed for fluorescence imaging as previously described (Gallego-Gomez et al., 2003; Martinez-Gutierrez et al., 2014). DENV E protein was stained with primary monoclonal anti-DENV envelope antibody (1:500, Millipore) and secondary fluorescent antibody Alexa 488 (1:1000, Molecular Probes). Nuclei were stained with Hoechst 33,258 (1:10000, Life-technologies). Fluorescence images were captured through Media Cybernetics Image Pro Plus software using an Olympus IX 81 epifluorescence microscope a 20X (UPlanSApo objective NA: 0.75). Five images per field were captured for each replicate at the indicated hpi. The area of E protein per cell was quantified using *ImageJ* software (Wayne Rasband, NIH, USA). Nuclei were regarded as cells, and data are expressed as the mean area of E protein labeling per cell ± standard error of three independent experiments. The Kolmogorov-Smirnov normality test was performed with SPSS (IBM).

2.4. Identification of cytokines and growth factors in culture supernatants of HMEC-1 cells

A multiplex immunoassay kit for 26 cytokines and growth factors was used according to the manufacturer's instructions (Milliplex® Map Human Cytokine/Chemokine Kit - Millipore Inc. USA) to evaluate the accumulation of IFNα2a, IL-1α, IL-1β, IL-3, IL-6, IL-7, IL-8, IL-15, IP-10, MCP-1, GRO, MCP-3, MDC, MIP-1α, MIP-1β, RANTES, Eotaxin, Fractalkine, TNF-α, TNF-β, G-CSF, GM-CSF, EGF, TGF-α, FGF-2 and VEGF in culture supernatants (conditioned media) of HMEC-1 cells at 1, 3, 12, 24 and 48 hpi. Serial dilutions (1:5; 10,000 into 3.2 pg/mL) of recombinant cytokines were used to construct standard curves from which cytokines and growth factor concentrations in culture supernatants were calculated. Fluorescence emitted from complexes was read with a Bio-Plex 200 System device (Bio-Rad Laboratories), and measures of median fluorescence intensity (MFI) were converted to pg/mL using Bioplex CFX manager software 5.0 (Biorad).

2.5. Cell migration assay

Culture supernatants (conditioned media) from DENV2-infected and mock-infected HMEC-1 cells at 1, 3, 12, 24 and 48 hpi were treated with UV light for virus inactivation. Then, 5×10^4 non-infected HMEC-1 cells were seeded with basal medium in the upper part of transwell inserts (pore 8-μm - Millipore Inc.USA) and inserted in 24-well plates with 600 μL of UV-treated conditioned media from different hpi as chemotactic stimulus.

Cell migration was allowed for 6 h and transwell inserts were processed as described (Justus et al., 2014). Fluorescence images from 5 fields (Olympus IX 81 epifluorescence microscope - 10X PlanApo objective/NA: 0.75) were captured with Image Pro Plus software, and nuclei (Hoechst stained) were counted using ImageJ software. Data are expressed as the mean ± standard error from three independent experiments. The statistical significance was assessed by two-way ANOVA for repeated measures.

2.6. Hierarchical cluster analysis (HCA)

The Past statistical package (3.18) was used to perform a hierarchical cluster analysis (HCA) over combined data sets from DENV-infected and mock-infected cells separately (Table S3). Average data (miRNA counts, cytokines, growth factors, %LDH and cell migration) were normalized with the "row normalize length" algorithm and HCA was performed by neighbour joining. The distance (Bray -Curtis dissimilarity-test) at which two cytokine clusters combine was represented by a horizontal line.

2.7. Total RNA extraction

Total RNA was isolated from DENV2-infected and mock-infected HMEC-1 cells at 3, 12, 24 and 48 h (n = 3) using the *Total RNA Purification Plus Kit* (NORGEN, Thorold, ON, Canada). RNA quality and quantity were measured using a Nanodrop spectrophotometer (ND-1000; Nanodrop Technologies, Wilmington, DE, USA). The RNA Integrity Number (RIN) was measured using a 2100 Bioanalyzer instrument (Agilent Inc). Only samples with RIN values > 7 were used for

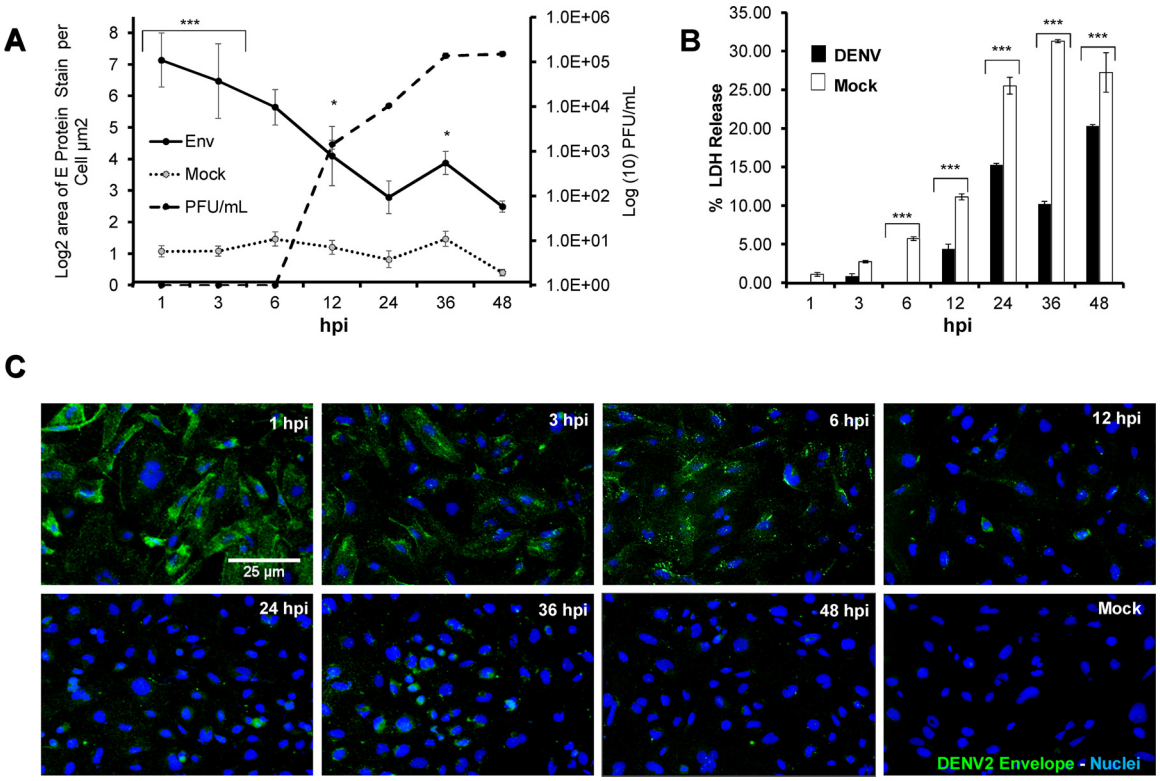

Fig. 1. DENV2 replication in HMEC-1 cells.
A. Area of DENV2 E protein staining per cell (black line) vs PFU release (dashed line) over time. Significant differences in E protein staining were observed at 1, 3, 6, 12 and 36 hpi (*** $P < 0.001$; * $P < 0.05$). **B**. LDH release in cell supernatants of DENV2-infected (black bars) and mock-infected HMEC-1 cells (white bars) at 1, 3, 6, 12, 24, 36 and 48 hpi. Data are expressed as the percentage of LDH release for three independent experiments (mean ± SE). Significant differences were evaluated using 2-way ANOVA for repeated measures (***$P < 0.001$). **C.** Fluorescence assays of DENV2-infected HMEC-1 cells. Images were taken at 20X magnification (UPlanSApo objective NA: 0.75) on an Olympus IX 81. Hpi: hours post-infection.

miRNA sequencing.

2.8. miRNA-seq library sequencing and analyzing

Library preparation and miRNA sequencing were performed at Exiqon, Denmark. microRNA NGS libraries were produced with the NEBNEXT® Multiplex Small RNA Library Prep Set for Illumina® (New England Biolabs Inc.) and sequenced on the Illumina NextSeq 500 system.

FASTQ files were evaluated for quality control using FastQC (0.11.2) and filtered for low quality and abundant short reads (less than 16 of nucleotide length); 3′ adapters (with length alignment greater than 25) were trimmed with fastx_clipper (0.0.13.2) (Martin, 2011). Filtered reads were mapped to the Human reference genome (hg19 - UCSC Genome Bioinformatics). Four alignment methods were compared (BWA (Li and Durbin, 2009), Bowtie, Bowtie2 (Langmead and Salzberg, 2012) and Segemehl (Hoffmann et al., 2009)) as a comprehensive mapping strategy for the recovery of accurate miRNA profiles of the sequenced samples. SAM files were processed to BAM format using SAMtools (Li et al., 2009). miRNA loci were filtered to reduce the miRbase's (v 20) annotation problems (Johnson et al., 2016). The over-representation of ambiguous mapped reads and the underestimation of rare dispersions was skipped out by using an automatic and non-redundant search strategy from (Tam et al., 2015). The performance of the tested aligners was contrasted by plotting the total reads counts per miRNA.

2.9. Differential expression analysis

Differential expression analyses were performed in the R statistical environment (v3.2.0) using EdgeR (v3.2.0) software (Bioconductor v2.12 repository). The time (hpi) and treatments (infection/mock) were considered as factors for constructing a design matrix to estimate dispersions according to the Cox-Reid profile-adjusted likelihood (CR) method. Four normalization methods count per million (CPM), upper quartile scaling (UQS), Trimmed Mean of M (TMM), Relative log expression (RLE)] were compared to perform differential expression analyses (Tam et al., 2015). The reads count in the design matrix were fitted to a generalized linear model (GLM) whereby differential expression of miRNAs between infected and mock-infected cells was tested. Log Fold changes (LogFC) greater than 0.59 or lower than -0.59, P values of 0.01 and a FDR less than 0.1 were used as thresholds to select the top set of differentially expressed miRNA candidates.

2.10. Network analysis

Validated miRNA-target interactions of the DE miRNAs (p-value < 0.01, LogFC infected/control < -0.59 < , LogFC infected/control > 0.59 and FDR < 0.1) after GLM-EdgeR analysis were identified with the online tool miRWalk 2.0 (http://zmf.umm.uni-heidelberg.de/apps/zmf/mirwalk2/), for constructing a list of genes regulated by the set of DE miRNAs (Table S3). The gene symbols were used as input in the ClueGo and Cluepedia applications from Cytoscape 3.2.0 (Bindea et al., 2009) to perform an analysis of functionally grouped annotation networks from the databases *REACTOME, GO* (*Biological Process[BP], Molecular Function[MF], Cellular Component[CC]*), *WikiPathways* and *KEGG*. Analysis parameters were as follows: statistic - hypergeometric, significance level - 0.01, multiple test adjustment - Benjamini & Hochberg (BH), minimum 30 genes for a category/cluster:, 5% of genes in a pathway leading group term: %Genes/Term.

3. Results

3.1. HMEC-1 cells do not support prolonged DENV2 infections

Virus growth curves from synchronized *DENV*2-infection assays demonstrate that after the inoculation, HMEC-1 cells release infectious virions around the 12 h, and the number of virions in culture supernatants gradually increased throughout the 48 h, demonstrating that DENV2 productively infects HMEC-1 cells. The staining of DENV E protein showed that about 100% of HMEC-1 cells were exposed to DENV2 at the first hpi (1 to 6 h), however, the staining gradually decreased throughout the 24 h with a slight recovery of fluorescence at 36 hpi (Fig. 1**A and C**). The low staining of DENV2 E protein at the later hours suggests that HMEC-1 cells do not support prolonged DENV infection as reported in other studies (Calvert et al., 2015; Talavera et al., 2004; Zamudio-Meza et al., 2009).

3.2. Lower LDH percentages in culture supernatants of DENV2-infected MECs

LDH accumulation in culture supernatants from infected and mock-infected cells was assessed to determine if *DENV*2 infection alters HMEC-1 viability by eliciting the loss of plasma membrane integrity. A lower percentage of LDH in culture supernatants of *DENV*2-infected HMEC-1 cells was observed between 6 to 48 hpi compared to time-matched mock-infected cells, suggesting that cytotoxicity was lower in DENV- infected HMEC-1 (Fig. 1B). It was reported that LDH assays failed to differentiate between cell death and growth inhibition (Smith et al., 2011), hence it was estimated the average number of nuclei per field as an indirect measure of cell proliferation. The amount of nuclei were equivalent and relatively constant between mock and DENV infected cells (**Fig. S1**). At 24 hpi, the number of nuclei doubled in both infected and mock-infected cells, suggesting that the cells replicated independently of the infection. However at 36 and 48 hpi, the number of nuclei returned back to the counts observed between 1 and 12 hpi. This observation could be understood as cell detachment by competition for space since this cell line normally growth as anchorage-dependent monolayers (Ades et al., 1992) and all the experiments were performed on confluent cultures. The major percentages of LDH release observed between 24 and 48 in both infected and mock-infected cells, could be due to LDH release from detached cells that was higher in mock-infected cells. Hence, the lower percentage of LDH released in DENV- infected cells was probably not due to a delayed cell cycle.

3.3. DENV2–infected MECs accumulate cytokines and growth factors

Chemokines and growth factors associated with *DENV*-induced pathology were evaluated in culture supernatants of *DENV*-infected and mock-infected HMEC-1 cells. No accumulation of IL-1α, IL-1β, IL-3, IL-7IL-15, TNF-α, TNF-β, IFN-α, MIP-1α, MIP-1β, Eotaxin, Fractalkine, MDC, IP-10 (CXCL10), EGF or VEGF was detected in the supernatants of infected and mock-infected HMEC-1 cells after 48 h, suggesting that *DENV* does not alter the expression of those soluble factors in this cell line. Among the soluble factors detected in culture supernatants, certain growth factors (FGF-2, TGF-α, GM-CSF and G-CSF), chemokines (GRO, IL-8: “CXC subfamily” and MCP1, MCP3 and RANTES “CC family”) and the innate inflammatory cytokine IL-6 were accumulated to higher levels in *DENV*2-infected cells compared to mock-infected cells (Fig. 2**A and B**). Interestingly, chemokines MCP1, IL-8 and GRO accumulated to higher levels in culture supernatants of infected cells compared to mock-infected cells at 6, 24, 36 and 48 hpi, but at 3 and 12 h, these factors were higher in mock-infected cells. Likewise, growth factors TGF-α and GM-CSF accumulated to higher levels in *DENV*2-infected cells at 6, 24, 36 and 48 hpi, while FGF-2 and MCP-3 levels were increased from 24 to 48 hpi, although levels were below those detected for MCP1, IL-8 and GRO. Finally, IL-6 was detected at higher levels in culture supernatants of infected cells from 6 to 48 h, while G-CSF and RANTES showed higher levels only at 48 h. Increases in these soluble factors were more pronounced at late hours post-infection. Taken together, these results suggest that *DENV*2 infection of HMEC-1 cells increases the accumulation of chemokines, growth factors and IL-6 in a time-dependent manner.

3.4. Conditioned media from DENV-infected MECs promote the migration of non-infected MECs

Conditioned media (CM) from *DENV*2-infected cells induced significant differences in the profile of HMEC-1 migration compared to mock-infected HMEC-1 cells, showing a biphasic migration pattern with peaks at 1, 6, 24 and 48 h and dips at 3, 12 and 36 h (Fig. 3). Curiously, CM from mock-infected cells induced the same biphasic pattern; however, only CM from mock-infected at 3 h induced a higher rate of migration compared to CM from infected cells. CM from *DENV*2-infected cells at 6, 24 and 48 h induced higher rates of cell migration compared to mock-infected cells.

3.5. The expression levels of six miRNAs are deregulated in DENV2-infected MECs

The abundance and distributions of reads mapped to miRNAs were plotted for each aligner (BWA, Bowtie, Bowtie2 and Segemehl) in order to show their influence to count reads by loci (**Fig. S2**) (Gutierrez-Díaz, 2018). The read counts generated by the four alignment methods and normalized by four normalization methods (upperquartile, CPM, TMM, and RLE) generated a set of six differentially expressed (DE) miRNAs after fitting to a Generalized Lineal Model (GLM). Specifically, let-7d-5p (Fig. 4A), miR-485-3p (Fig. 4B), miR-320e (Fig. 4E), miR-4498 (Fig. 4F), and miR-98-5p (Fig. 4C) showed a continuous increase in the expression levels in DENV-infected cells up to 24 hpi and an inverse behavior in the mock-infected cells. Furthermore, an opposite behavior was observed for the miR-27a (Fig. 4D) which expression rate decreased during 3–24 hpi in DENV-infected cells compared to mock condition.

It was remarkable that the differential expression of all these miRNAs was not detected by the same computational strategy, for instance, DE of miR-320e and miR-4498 was detected by Bowtie-RLE while miR-27a-5p was detected by Segemehl-upperquartile strategy (**Table S1**).

Finally, an additional set of miRNAs tended to be differentially expressed, although they were outside of the LogFC threshold (**Fig. S3** and **Table S2**).

3.6. DENV-infection alters association patterns of miRNAs and soluble factors

In order to detect potential patterns of soluble factors and miRNAs associated with cell migration during DENV-infection, hierarchical clustering analyses were separately performed on DENV-infected and mock-infected cells by combining all the data sets (miRNA counts, DENV release, cytokines, growth factors, %LDH and cell migration) (**Table S3**). In (Fig. 5A) the dendrograms displayed different gathering patterns between infected and mock-infected data sets. In the mock-infected dataset, cell migration was clustered with miR-4498 and miR-320, while soluble factors and the remaining miRNAs gather in independent clusters. For the DENV-infected case (Fig. 5B), two larger and more discrete clusters are observed, in the first one, DENV-release was closely associated to G-CSF, RANTES, followed by GRO, FGF-2, IL-8 and MCP-1. The second cluster was formed by a narrow subgroup between miR-485-3p, miR-98-5p and let-7d-5p followed by miR-320e, migration, TGF-α, miR-4498, IL-6, GM-CSF, %LDH and MCP-3. Importantly, as observed for the mock-infected dataset, the expression patterns of miR-4498 and miR-320e appear to be more associated to

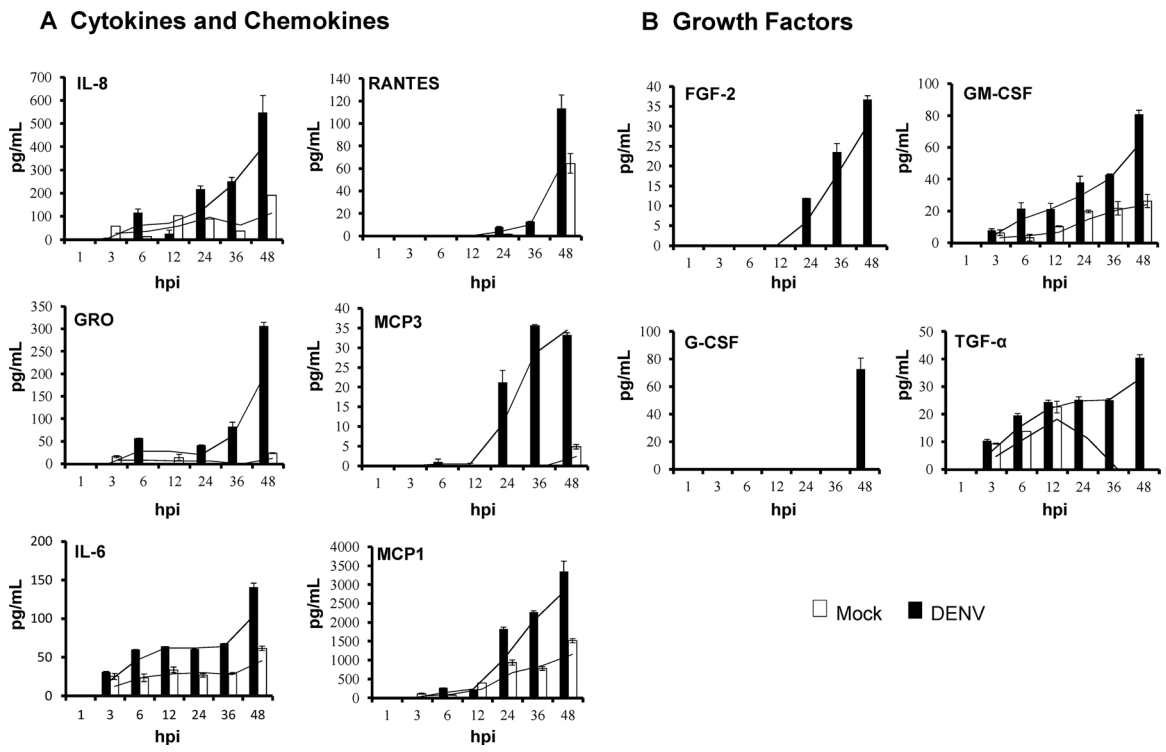

Fig. 2. Quantification of cytokines-growth factors in culture supernatants.
Cytokines-chemokines (**A**), and growth factor (**B**) levels in DENV2-infected (black bars) and mock-infected (white bars) HMEC-1 cells at 48 hpi. Significant differences were evaluated using 2-way ANOVA for repeated measures in three independent assays. * $P < 0.05$; ** $P < 0.01$; *** $P < 0.001$.

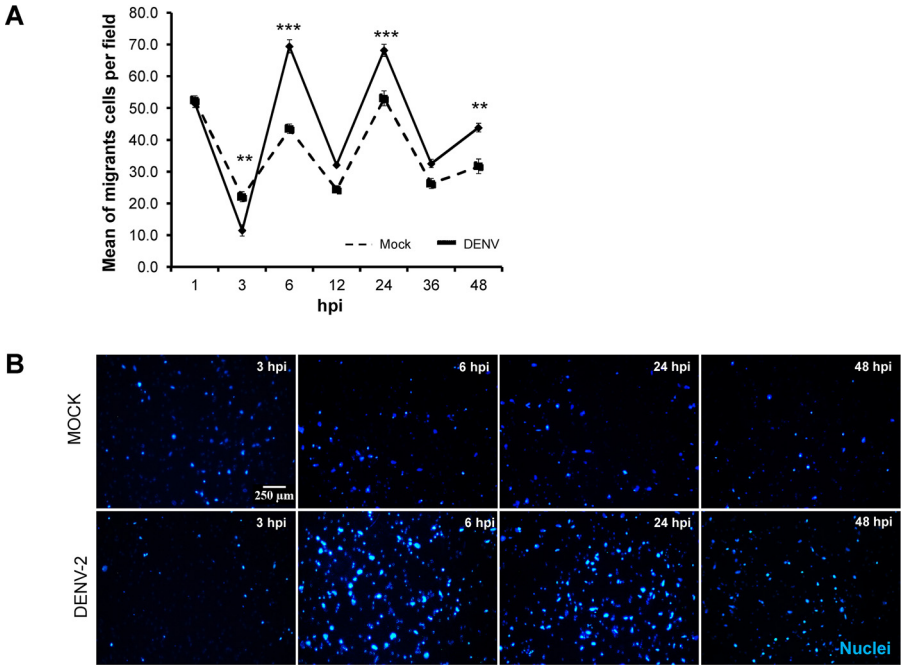

Fig. 3. HMEC-1 cell migration in response to culture supernatants.
A. HMEC-1 cells were allowed to migrate during 6 h in response to conditioned media (1 to 48 hpi) from DENV2-infected (continuous line) and mock-infected (dashed line) cells. **B.** Representative images of migrating cells at the significantly different time points. Data are expressed as the mean of cells per field (mean ± SE). Nuclei were stained with Hoechst 33,258. Significant differences were evaluated by 2-way ANOVA for repeated measures in three independent assays. *$P < 0.05$; **$P < 0.01$; *** $P < 0.001$.

migration patterns among the entire set of miRNAs. Furthermore, TGF-α expression patterns were closer together with migration patterns, thus the increases in cell migration observed in the context of DENV-infection appear to be more associated to the increases in TGF-α.

3.7. Potentially altered genes by miRNAs in DENV2-infected MECs regulate cell migration, vasculature development and angiogenesis

After look for experimentally validated miRNA-target interactions at miRWalk database, a total list of 1670 genes were potentially targeted by the set of miRNAs deregulated in DENV-infected MECs (**Table S4**), together, those genes are involved 1070 biological pathways (**Table S5**).

Notably, in concordance with the transwell migration assays that suggested cell migration augments promoted by *DENV*2 infection, network analysis suggested a group of biological processes associated with processes involved in cell migration including, *positive regulation of cell migration*, *positive regulation of locomotion, regulation of cellular*

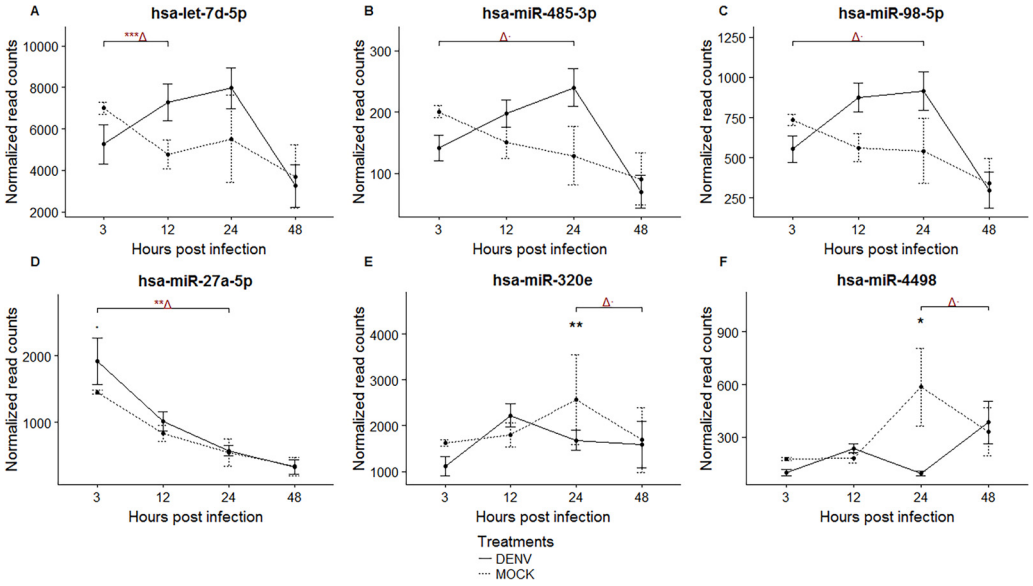

Fig. 4. Differentially expressed miRNAs in DENV2-infected HMEC-1 cells.

Mature miRNAs with P < 0.01, FDR = < 0.1 (.), < 0.05 (*), < 0.01(**) and < 0.001(***), and LogFC < -0.59 or > 0.59 relative to mock-infected control were considered as statistically significant DE miRNAs (**A-F**). There are two kinds of contrast, paired hours post-infection (DENV vs mock-infected) and the change in the number of read counts over time (DENV vs mock-infected), for instance, miR-27a-5p (**D**) was upregulated at 3 hpi and down-regulated between 3 and 24 hpi (**Δ), which means that the decay of the miR-27a-5p was more pronounced in DENV2-infected cells. The opposite behavior was observed for miR-98-5p.

component movement and positive regulation of cell adhesion (Fig. 6A). In addition other cellular processes associated to vascular developmental processes such as *vasculature development, blood vessel morphogenesis* and *angiogenesis* where suggested by the network analysis as potential processes affected by the deregulated miRNAs in DENV-infected MECs (Fig. 6B).

4. Discussion

DENV infection of humans is associated with an unregulated secretion of various soluble mediators such as chemokines, proinflammatory-vasoactive cytokines/chemokines, growth factors and complement activators, among others. Studies in multiple organs of human fatal cases suggest that endothelial cells are poorly infected *in vivo* (Jessie et al., 2004; Povoa et al., 2014). However, *in vitro* studies suggest that *DENV*-infected ECs are important sources of cytokines and chemokines that activate immune responses leading to the destabilization of the endothelial barrier (Calvert et al., 2015; Dalrymple and Mackow, 2012; Talavera et al., 2004).

In this work, HMEC-1 cells were productively infected by DENV2, however the decrease of DENV2 envelope stain at late hpi (Fig. 1A and C) suggest a restriction of viral replication in a time-dependent manner,

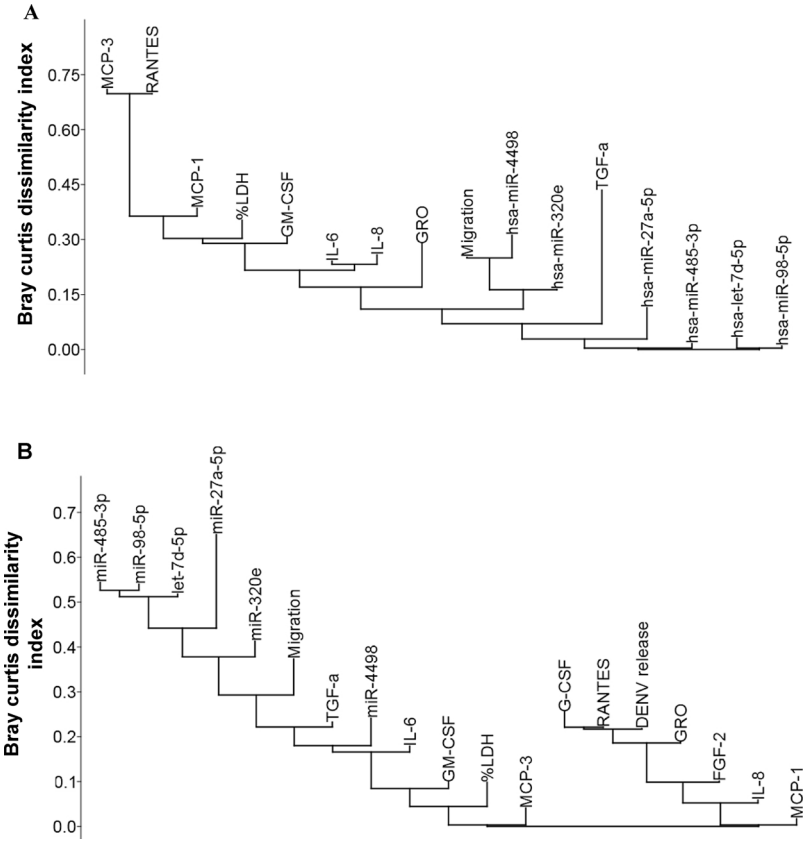

Fig. 5. Unsupervised hierarchical clustering of the expression of soluble factors, miRNAs and migration of MECs.

Clustering of cytokines, growth factors, %LDH release, miRNA counts and cell migration in mock infected (**A**) and DENV-infected (**B**) MECs. Cell migration formed a discrete cluster with TGF-α and five miRNAs (**B**) in DENV-infected MECs.

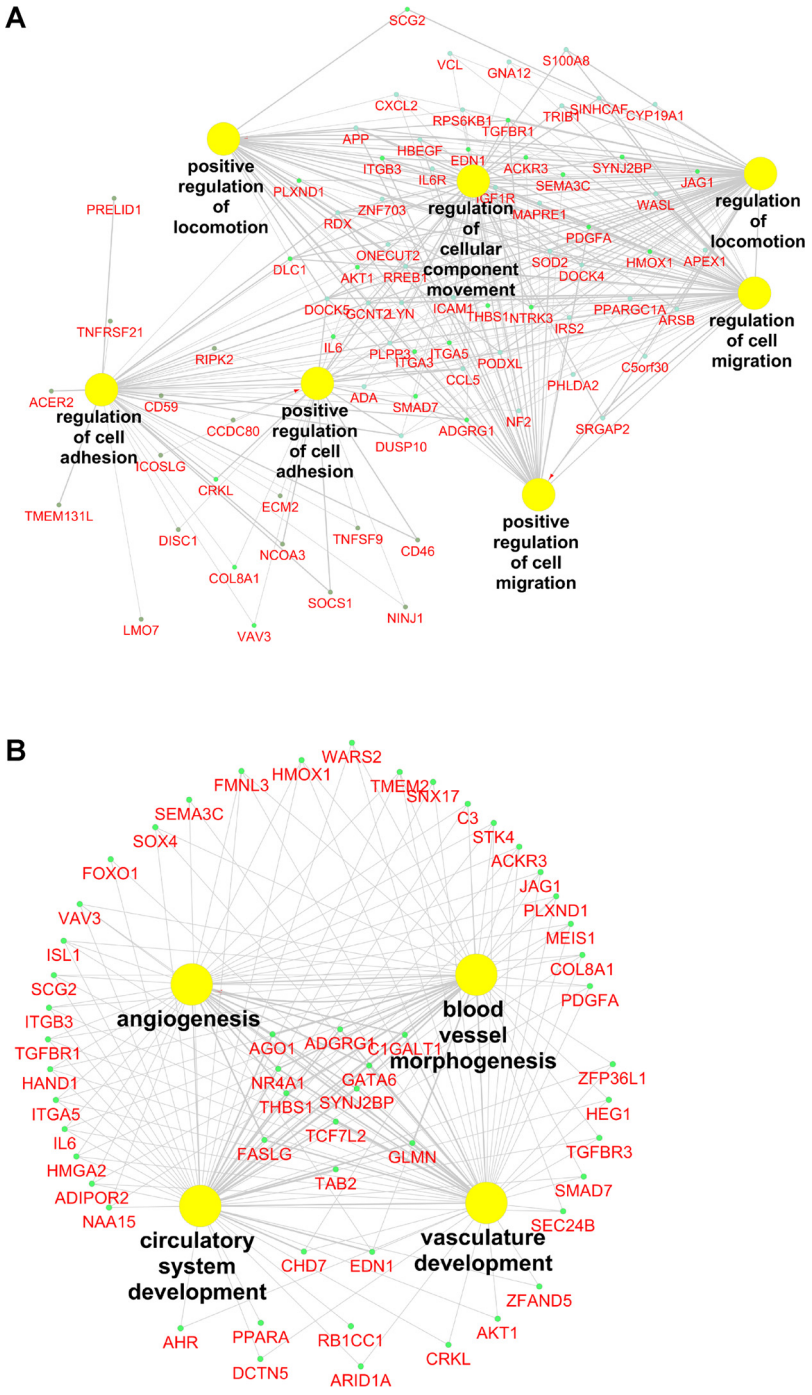

Fig. 6. Biological processes potentially altered in DENV2-infected HMEC-1 cells.
Functional network analysis depicting the biological processes regulated by the target genes (from miRWalk "Validated miRNA-target interactions" module) of the deregulated miRNAs in DENV-infected MECs. **A**. Network of genes that regulate biological processes involved in cell migration. **B**. Network of genes that regulate biological processes involved in vascular development. Term P-Values corrected with bonferroni step down were between 1×10^{-9} and 9×10^{-18} and summarized in the table S4.

consistent with other studies (Dalrymple and Mackow, 2012) and not explained by a loss in the cell viability (Fig. 1B).

Importantly, conditioned media from these cells had increased levels of chemokines (GRO, IL-8, MCP-1, MCP3 and RANTES), growth factors (FGF-2, TGF-α, GM-CSF, G-CSF) as well as IL-6. Except for MCP-3, GRO, and TGF-α, all these factors have been associated with vascular leakage in severe dengue (Bozza et al., 2008; Kumar et al., 2012; Tramontini Gomes de Sousa Cardozo et al., 2017). Furthermore, there are no studies that investigate if DENV induces changes in the levels of GRO, TGF-α, FGF-2 and MCP-3 in MECs. Thus, this is the first evidence that ECs may be important sources of these factors during *DENV* infections in human MECs.

FGF-2, TGF-α and GM-CSF are reported to be potent stimulators of EC migration, cell survival and angiogenesis that activate PI3K/AKT and MAPK pathways (Dorey and Amaya, 2010; Lopez et al., 2010). Several studies have also reported that the chemokines GRO, IL-8 and MCP-1 act as chemotactic factors for ECs during angiogenesis (Keeley et al., 2008). In fact, the migration assays performed in this study suggest that *DENV*-infected MECs release soluble mediators that increase the migration of non-infected MECs. The increase of pro-

migratory/angiogenic cytokines and growth factors in conditioned media from DENV-infected MECs suggest that the highest levels of cell migration may be due to the increase in the concentration of some of these soluble factors (Fig. 3). However, additional studies should be directed to determine whether these factors are involved in the augments of cell migration in this context.

It was also remarkable that DENV- and mock-infected MECs exhibited the same oscillating migration pattern over time, although the intensity of the migration peaks was greater in response to conditioned media from infected cells (Fig. 3). Although those data do not provide evidence to explain the nature of the observed oscillatory patterns, it suggest that DENV infection may alter the intensity of the oscillations in the cell migration and the accumulation of soluble pro-migratory factors in the culture supernatants. Nevertheless, further experiments must be performed to test this approach.

Thus, the *DENV*-induced vascular dysfunction observed in SD disease could be thought in part as an acute MECs migratory disorder due to MECs migration requires the disruption of inter-endothelial junctions, such as tight and adherents junctions, generating spaces for vascular leakage (Nagy et al., 2012).

Similar to the results observed using conditioned media from *DENV*-infected HMEC-1 cells, miRNA-seq analyses revealed a small group of differentially expressed miRNAs whose validated gene targets from miRWalk database alter cellular processes involved in cell migration and vascular development as suggested by network analyses (Fig. 6). Accordingly, recent evidence from transcriptomic analyses has shown that DENV is able to alter the expression of genes involved in migratory responses in neuronal cells (Zhang et al., 2016). However, the proposed gene targets of the DE miRNAs are tentative and additional experiments (i.e., transfection with the candidate miRNAs, specific blockade whit anti-miRs, and luciferase reporter assays) are required to validate the migratory phenotype and to demonstrate if these genes are actually targeted in this context. Therefore, some evidence about the role of these miRNAs in the regulation of genes involved in cell migration is discussed below.

Accordingly, the upregulation of miR-27a-5p negatively impacts the cell migration, by targeting the AKT1 gene, a positive regulator of endothelial cell migration (Wu et al., 2013; Yang et al., 2018). miR-320 was reported as an anti-angiogenic microRNA that suppressed the migration, adhesion and tube formation of vascular endothelial cells by targeting NRP1 an important regulator of angiogenesis (Wu et al., 2014), this miRNA was downregulated at 24 h in DENV-infected MECs (Fig. 4E).

Three miRNAs (miR-98-5p, miR-485-3p-3p and miR-4498) not previously associated with DENV infection were differentially expressed in DENV-infected cells (Fig. 4B, C and F). It was reported that miR-98-5p and miR-485-3p-3p regulate the cell migration in different contexts. For instance, hsa-miR-98-5p (a member of hsa-let-7 family) target into thrombospondin-1 (THBS1) an anti-angiogenic protein and a strong activator of Epithelial-to-Mesenchymal Transition (EMT) in which cells acquire a migratory phenotype (Jayachandran et al., 2014; Kuehbacher et al., 2007). This miRNA also targets into TGFBR1 and TGFBR3 which are receptors for the transforming growth factor B another strong activator of EMT (Chen et al., 2012), those receptors were enriched in our network analysis (Fig. 6). On the other hand, hsa-miR-485-3p-3p can suppress the cell migration by targeting PGC-1α (Lou et al., 2016).

There was another group of six miRNAs (miR-125-5p, miR-155-5p, miR-221-3p, miR-24-3p. miR-378-3p, miR-409-3p and miR-92b-3p) which yielded good P and FDR values but not significant LogFC values (Table S3 and Fig. S3). However, changes in the expression dynamics of these miRNAs are supported by previous studies with miRNA profiling during DENV-infection providing insights of its potential roles in the vascular pathology of DENV (Aloia et al., 2015; Ouyang et al., 2016; Qi et al., 2013; Tambyah et al., 2016).

In a previous computational identification of *DENV* microRNA-like structures performed by our group (Ospina-Bedoya et al., 2014) it was predicted a group of proteins involved in angiogenesis and chemotaxis (such as fibroblast growth factor receptor 2 [FGFR]), thymidine phosphorylase [TYMP], protein phosphatase 2, regulatory subunit B' and gamma [PPP2R5C]) among the potential targets of *DENV*2-miR170 and *DENV*2-miR14, suggesting a potential role for *DENV* microRNA-like structures in regulating vascular remodeling processes.

The fact that miRNAs commonly exert their functions through gene silencing suggests a negative regulatory mechanism for these processes in *DENV*2-infected HMEC-1 cells. In addition, it is possible that the miRNAs detected in our study were up-regulated or down-regulated as a "fine-tuning" mechanism to counteract the migratory stimuli promoted by the soluble factors detected in the cell supernatants. For instance, it has been reported that miR-379 counteracts the overexpression of the ABCC2 protein in HepG2 cells in the presence of the transcriptional stimulator rifampicin (Haenisch et al., 2011). Thus, the identified miRNAs in DENV-infected HMEC-1 cells could be acting in a similar manner.

In conclusion, the analyses of cytokines/growth factors and microRNAs expression indicate that miRNAs are likely an important driving force in the release of cytokines, chemokines and growth factors that promote microvascular EC migration. These results provide a new insight that would encourage researchers to conduct new studies in the context of DENV-infection to validate the expression of the genes predicted to be targets of miRNAs involved in cell migration and vascular development.

Authors' contributions

DAA, EOG, CIBS and JCGG conceived and designed the experiments, DAA and EOG performed all the experiments with DENV-infected cells. AAG, APG, CBIS and DAA were involved in computational analyses. All authors participated in the manuscript preparation, read and approved the final manuscript.

Competing interests

The authors have declared no competing interests.

Acknowledgements

This research was supported by the Administrative Department of Science, Technology and Innovation – COLCIENCIAS grant 111554531621(JCG-G). Micro-RNAseq data analysis was supported by an equipment donation from the German Academic Exchange Service-DAAD (Sachmittel programm 226.104401.329) to the Faculty of Science at the Universidad Nacional de Colombia. AAG was supported by the scholarship graduate program at the Universidad Nacional de Colombia, Sede Bogotá Resolución 498-2015, acta 13 October 23th 2015.]

Appendix A. Supplementary data

Supplementary material related to this article can be found, in the online version, at doi:https://doi.org/10.1016/j.virusres.2018.10.018.

References

Ades, E.W., Candal, F.J., Swerlick, R.A., George, V.G., Summers, S., Bosse, D.C., Lawley, T.J., 1992. HMEC-1: establishment of an immortalized human microvascular endothelial cell line. J. Invest. Dermatol. 99 (6), 683–690.

Aloia, A.L., Abraham, A.M., Bonder, C.S., Pitson, S.M., Carr, J.M., 2015. Dengue virus-induced inflammation of the endothelium and the potential roles of sphingosine Kinase-1 and MicroRNAs. Mediators Inflamm. 2015, 509306.

Bäck, A.T., Lundkvist, Å., 2013. Dengue viruses – an overview. Infect. Ecol. Epidemiol. 3. https://doi.org/10.3402/iee.v3403i3400.19839.

Bhatt, S., Gething, P.W., Brady, O.J., Messina, J.P., Farlow, A.W., Moyes, C.L., Drake, J.M., Brownstein, J.S., Hoen, A.G., Sankoh, O., Myers, M.F., George, D.B., Jaenisch,

T., Wint, G.R., Simmons, C.P., Scott, T.W., Farrar, J.J., Hay, S.I., 2013. The global distribution and burden of dengue. Nature 496 (7446), 504–507.
Bindea, G., Mlecnik, B., Hackl, H., Charoentong, P., Tosolini, M., Kirilovsky, A., Fridman, W.H., Pages, F., Trajanoski, Z., Galon, J., 2009. ClueGO: a Cytoscape plug-in to decipher functionally grouped gene ontology and pathway annotation networks. Bioinformatics 25 (8), 1091–1093.
Bozza, F.A., Cruz, O.G., Zagne, S.M., Azeredo, E.L., Nogueira, R.M., Assis, E.F., Bozza, P.T., Kubelka, C.F., 2008. Multiplex cytokine profile from dengue patients: MIP-1beta and IFN-gamma as predictive factors for severity. BMC Infect. Dis. 8, 86.
Calvert, J.K., Helbig, K.J., Dimasi, D., Cockshell, M., Beard, M.R., Pitson, S.M., Bonder, C.S., Carr, J.M., 2015. Dengue virus infection of primary endothelial cells induces innate immune responses, changes in endothelial cells function and is restricted by interferon-stimulated responses. J. Interferon Cytokine Res 35 (8), 1–12.
Chen, P.Y., Qin, L., Barnes, C., Charisse, K., Yi, T., Zhang, X., Ali, R., Medina, P.P., Yu, J., Slack, F.J., Anderson, D.G., Kotelianski, V., Wang, F., Tellides, G., Simons, M., 2012. FGF regulates TGF-beta signaling and endothelial-to-mesenchymal transition via control of let-7 miRNA expression. Cell Rep. 2 (6), 1684–1696.
Dalrymple, N.A., Mackow, E.R., 2012. Endothelial cells elicit immune-enhancing responses to dengue virus infection. J. Virol. 86 (12), 6408–6415.
Dorey, K., Amaya, E., 2010. FGF signalling: diverse roles during early vertebrate embryogenesis. Development 137 (22), 3731–3742.
Gallego-Gomez, J.C., Risco, C., Rodriguez, D., Cabezas, P., Guerra, S., Carrascosa, J.L., Esteban, M., 2003. Differences in virus-induced cell morphology and in virus maturation between MVA and other strains (WR, Ankara, and NYCBH) of vaccinia virus in infected human cells. J. Virol. 77 (19), 10606–10622.
Gutierrez-Díaz, A.A., 2018. Detección automatizada de pequeños fragmentos derivados de RNAs no-codificantes expresados diferencialmente frente a la infección del virus Dengue. Universidad Nacional de Colombia.
Haenisch, S., Laechelt, S., Bruckmueller, H., Werk, A., Noack, A., Bruhn, O., Remmler, C., Cascorbi, I., 2011. Down-regulation of ATP-binding cassette C2 protein expression in HepG2 cells after rifampicin treatment is mediated by microRNA-379. Mol. Pharmacol. 80 (2), 314–320.
Hoffmann, S., Otto, C., Kurtz, S., Sharma, C.M., Khaitovich, P., Vogel, J., Stadler, P.F., Hackermuller, J., 2009. Fast mapping of short sequences with mismatches, insertions and deletions using index structures. PLoS Comput. Biol. 5 (9) e1000502.
Jayachandran, A., Anaka, M., Prithviraj, P., Hudson, C., McKeown, S.J., Lo, P.H., Vella, L.J., Goding, C.R., Cebon, J., Behren, A., 2014. Thrombospondin 1 promotes an aggressive phenotype through epithelial-to-mesenchymal transition in human melanoma. Oncotarget 5 (14), 5782–5797.
Jessie, K., Fong, M.Y., Devi, S., Lam, S.K., Wong, K.T., 2004. Localization of dengue virus in naturally infected human tissues, by immunohistochemistry and in situ hybridization. J. Infect. Dis. 189 (8), 1411–1418.
Johnson, N.R., Yeoh, J.M., Coruh, C., Axtell, M.J., 2016. Improved placement of multi-mapping small RNAs. G3 Bethesda (Bethesda) 6 (7), 2103–2111.
Justus, C.R., Leffler, N., Ruiz-Echevarria, M., Yang, L.V., 2014. In vitro cell migration and invasion assays. J. Vis. Exp. 88.
Keeley, E.C., Mehrad, B., Strieter, R.M., 2008. Chemokines as mediators of neovascularization. Arterioscler. Thromb. Vasc. Biol. 28 (11), 1928–1936.
Kuehbacher, A., Urbich, C., Zeiher, A.M., Dimmeler, S., 2007. Role of Dicer and Drosha for endothelial microRNA expression and angiogenesis. Circ. Res. 101 (1), 59–68.
Kumar, Y., Liang, C., Bo, Z., Rajapakse, J.C., Ooi, E.E., Tannenbaum, S.R., 2012. Serum proteome and cytokine analysis in a longitudinal cohort of adults with primary dengue infection reveals predictive markers of DHF. PLoS Negl. Trop. Dis. 6 (11), e1887.
Langmead, B., Salzberg, S.L., 2012. Fast gapped-read alignment with Bowtie 2. Nat. Methods 9 (4), 357–359.
Li, H., Durbin, R., 2009. Fast and accurate short read alignment with Burrows-Wheeler transform. Bioinformatics 25 (14), 1754–1760.
Li, H., Handsaker, B., Wysoker, A., Fennell, T., Ruan, J., Homer, N., Marth, G., Abecasis, G., Durbin, R., Genome Project Data Processing, S, 2009. The sequence Alignment/Map format and SAMtools. Bioinformatics 25 (16), 2078–2079.
Liu, S., Chen, L., Zeng, Y., Si, L., Guo, X., Zhou, J., Fang, D., Zeng, G., Jiang, L., 2016. Suppressed expression of miR-378 targeting gzmb in NK cells is required to control dengue virus infection. Cell. Mol. Immunol. 13 (5), 700–708.
Lopez, A.F., Hercus, T.R., Ekert, P., Littler, D.R., Guthridge, M., Thomas, D., Ramshaw, H.S., Stomski, F., Perugini, M., D'Andrea, R., Grimbaldeston, M., Parker, M.W., 2010. Molecular basis of cytokine receptor activation. IUBMB Life 62 (7), 509–518.
Lou, C., Xiao, M., Cheng, S., Lu, X., Jia, S., Ren, Y., Li, Z., 2016. MiR-485-3p and miR-485-5p suppress breast cancer cell metastasis by inhibiting PGC-1alpha expression. Cell Death Dis. 7, e2159.
Malavige, G.N., Ogg, G.S., 2017. Pathogenesis of vascular leak in dengue virus infection. Immunology 151 (3), 261–269.
Martin, M., 2011. Cutadapt removes adapter sequences from high-throughput sequencing reads. EMBnet J. 17 (1).
Martinez-Gutierrez, M., Correa-Londono, L.A., Castellanos, J.E., Gallego-Gomez, J.C., Osorio, J.E., 2014. Lovastatin delays infection and increases survival rates in AG129 mice infected with dengue virus serotype 2. PLoS One 9 (2), e87412.
Michels, M., van der Ven, A.J., Djamiatun, K., Fijnheer, R., de Groot, P.G., Griffioen, A.W., Sebastian, S., Faradz, S.M., de Mast, Q., 2012. Imbalance of angiopoietin-1 and angiopoetin-2 in severe dengue and relationship with thrombocytopenia, endothelial activation, and vascular stability. Am. J. Trop. Med. Hyg. 87 (5), 943–946.
Nagy, J.A., Dvorak, A.M., Dvorak, H.F., 2012. Vascular hyperpermeability, angiogenesis, and stroma generation. Cold Spring Harb. Perspect. Med. 2 (2), a006544.
Ospina-Bedoya, M., Campillo-Pedroza, N., Franco-Salazar, J.P., Gallego-Gomez, J.C., 2014. Computational identification of dengue virus MicroRNA-Like structures and their cellular targets. Bioinform. Biol. Insights 8, 169–176.
Ouyang, X., Jiang, X., Gu, D., Zhang, Y., Kong, S.K., Jiang, C., Xie, W., 2016. Dysregulated serum MiRNA profile and promising biomarkers in dengue-infected patients. Int. J. Med. Sci. 13 (3), 195–205.
Pepini, T., Gorbunova, E.E., Gavrilovskaya, I.N., Mackow, J.E., Mackow, E.R., 2010. Andes virus regulation of cellular microRNAs contributes to hantavirus-induced endothelial cell permeability. J. Virol. 84 (22), 11929–11936.
Povoa, T.F., Alves, A.M., Oliveira, C.A., Nuovo, G.J., Chagas, V.L., Paes, M.V., 2014. The pathology of severe dengue in multiple organs of human fatal cases: histopathology, ultrastructure and virus replication. PLoS One 9 (4), e83386.
Qi, Y., Li, Y., Zhang, L., Huang, J., 2013. microRNA expression profiling and bioinformatic analysis of dengue virusinfected peripheral blood mononuclear cells. Mol. Med. Rep. 7 (3), 791–798.
Smith, S.M., Wunder, M.B., Norris, D.A., Shellman, Y.G., 2011. A simple protocol for using a LDH-Based cytotoxicity assay to assess the effects of death and growth inhibition at the same time. PLoS One 6 (11), e26908.
Srikiatkhachorn, A., Wichit, S., Gibbons, R.V., Green, S., Libraty, D.H., Endy, T.P., Ennis, F.A., Kalayanarooj, S., Rothman, A.L., 2012. Dengue viral RNA levels in peripheral blood mononuclear cells are associated with disease severity and preexisting dengue immune status. PLoS One 7 (12), e51335.
St John, A.L., Abraham, S.N., Gubler, D.J., 2013. Barriers to preclinical investigations of anti-dengue immunity and dengue pathogenesis. Nat. Rev. Microbiol. 11 (6), 420–426.
Talavera, D., Castillo, A.M., Dominguez, M.C., Gutierrez, A.E., Meza, I., 2004. IL8 release, tight junction and cytoskeleton dynamic reorganization conducive to permeability increase are induced by dengue virus infection of microvascular endothelial monolayers. J. Gen. Virol. 85 (Pt 7), 1801–1813.
Tam, S., Tsao, M.S., McPherson, J.D., 2015. Optimization of miRNA-seq data preprocessing. Brief Bioinform. 16 (6), 950–963.
Tambyah, P.A., Ching, C.S., Sepramaniam, S., Ali, J.M., Armugam, A., Jeyaseelan, K., 2016. microRNA expression in blood of dengue patients. Ann. Clin. Biochem. 53 (Pt 4), 466–476.
Tramontini Gomes de Sousa Cardozo, F., Baimukanova, G., Lanteri, M.C., Keating, S.M., Moraes Ferreira, F., Heitman, J., Pannuti, C.S., Pati, S., Romano, C.M., Cerdeira Sabino, E., 2017. Serum from dengue virus-infected patients with and without plasma leakage differentially affects endothelial cells barrier function in vitro. PLoS One 12 (6), e0178820.
Tu, T., Zhang, C., Yan, H., Luo, Y., Kong, R., Wen, P., Ye, Z., Chen, J., Feng, J., Liu, F., Wu, J.Y., Yan, X., 2015. CD146 acts as a novel receptor for netrin-1 in promoting angiogenesis and vascular development. Cell Res. 25 (3), 275–287.
WHO, 2009. Dengue: Guidelines for Diagnosis, Treatment, Prevention and Control. World Health Organization. World Health Organization, Geneva, Switzerland: WHO 2009.
WHO, 2017. Dengue Control: Epidemiology, vol. 2017 World Healt Organization.
Wu, F., Yang, Z., Li, G., 2009. Role of specific microRNAs for endothelial function and angiogenesis. Biochem. Biophys. Res. Commun. 386 (4), 549–553.
Wu, X., Bhayani, M.K., Dodge, C.T., Nicoloso, M.S., Chen, Y., Yan, X., Adachi, M., Thomas, L., Galer, C.E., Jiffar, T., Pickering, C.R., Kupferman, M.E., Myers, J.N., Calin, G.A., Lai, S.Y., 2013. Coordinated targeting of the EGFR signaling axis by microRNA-27a*. Oncotarget 4 (9), 1388–1398.
Wu, Y.Y., Chen, Y.L., Jao, Y.C., Hsieh, I.S., Chang, K.C., Hong, T.M., 2014. miR-320 regulates tumor angiogenesis driven by vascular endothelial cells in oral cancer by silencing neuropilin 1. Angiogenesis 17 (1), 247–260.
Yang, W., Tang, K., Wang, Y., Zan, L., 2018. MiR-27a-5p increases steer fat deposition partly by targeting calcium-sensing receptor (CASR). Sci. Rep. 8 (1), 3012.
Zamudio-Meza, H., Castillo-Alvarez, A., Gonzalez-Bonilla, C., Meza, I., 2009. Cross-talk between Rac1 and Cdc42 GTPases regulates formation of filopodia required for dengue virus type-2 entry into HMEC-1 cells. J. Gen. Virol. 90 (Pt 12), 2902–2911.
Zhang, F., Hammack, C., Ogden, S.C., Cheng, Y., Lee, E.M., Wen, Z., Qian, X., Nguyen, H.N., Li, Y., Yao, B., Xu, M., Xu, T., Chen, L., Wang, Z., Feng, H., Huang, W.K., Yoon, K.J., Shan, C., Huang, L., Qin, Z., Christian, K.M., Shi, P.Y., Xu, M., Xia, M., Zheng, W., Wu, H., Song, H., Tang, H., Ming, G.L., Jin, P., 2016. Molecular signatures associated with ZIKV exposure in human cortical neural progenitors. Nucleic Acids Res. 44 (18), 8610–8620.
Zhu, X., He, Z., Hu, Y., Wen, W., Lin, C., Yu, J., Pan, J., Li, R., Deng, H., Liao, S., Yuan, J., Wu, J., Li, J., Li, M., 2014. MicroRNA-30e* suppresses dengue virus replication by promoting NF-kappaB-dependent IFN production. PLoS Negl. Trop. Dis. 8 (8), e3088.